4.5.2 Optimization of Etching parameters

The parameters for the etching of SiO_2 were investigated utilizing the alternate gas supply method developed in section 4.5.1. For the convenience of description, we omit the specific demonstration of O_2 supply recipe from now on. Since the final goal for the whole optimization experiments is to fabricate the III-nitrides 2D PC with periodicity of 150 nm or smaller, the optimal fabrication condition for SiO_2 mask should fulfill the following condition:

1. Sufficient thickness for the subsequent pattern transfer into AlN layer.
2. Abrupt vertical etching profile of the airhole.

SiO_2 films with three different thickness values of 130 nm, 195 nm and 260 nm were used for experiments. Mention again the parameters to be investigated are source power, bias power, gas pressure and gas ratio. Among these parameters, we first set the bias power to 300 W that is the maximum value of our RIE equipment, expecting good vertical profile of airholes. Since under high bias power environment, the perpendicular nature of the ion bombardment energy will be enhanced, leading to the improved anisotropic etching. With the bias power fixed to 300 W, we changed the source power from 100 W to 200 W with an increase. Note that one must considerate both source power and bias power upon the seeking for optimal dry etching process. Since many results can be achieved by either a change of source power or that of bias power, which means the etching profile is influenced to a great extent by the competition of source power and bias power. In other words, adjustment of the plasma flux by controlling source power can result in the similar consequence with the adjustment of ion-bombardment effect by controlling bias power. In this case, we fixed the bias power to 300 W and looked for the most suitable source power value. As the result, we found under the condition of source power 125 W and bias power 300 W, most abrupt vertical etching profile was achieved. Therefore, we fixed the source and bias power value to 125 W and 300 W, respectively and moved on to the investigation of gas pressure.

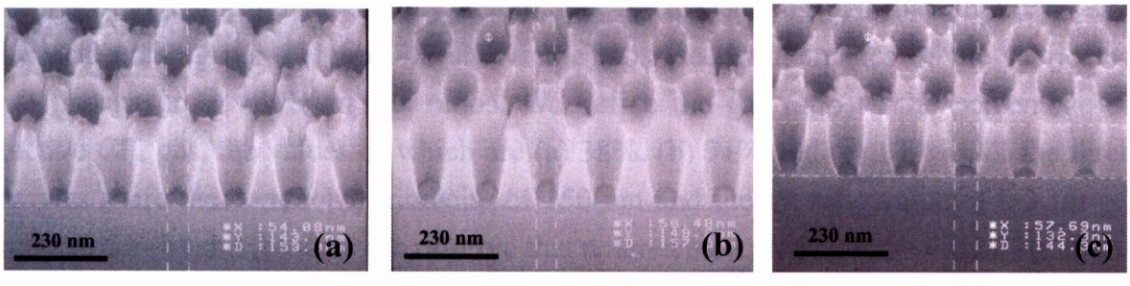

Fig. 4.7 Cross-sectional SEM images of the SiO2 masks fabricated under different gas pressure: (a) 0.25 Pa, (b) 0.75 Pa, and (c) 1.25 Pa. The periodicity is 150 nm and the r/a ratio is 0.25.

The optimization of gas pressure was carried out from the starting condition as: **Source power 125 W, bias power 300 W, CF_4 5 cc, Ar 8 cc and gas pressure 0.75 Pa**. The pressure of gases was changed between 0.25 Pa to 1.25 Pa with an increase by 0.5 Pa. Figure 4.7 shows the cross-sectional images of the fabricated SiO_2 masks under different pressure values of (a) 0.25 Pa, (b) 0.75 Pa and (c) 1.25 Pa. All the three samples share the common periodicity of 150 nm and r/a ratio of 0.25.

We observed significant deterioration on the vertical profile of airholes under the lowest pressure value of 0.25 Pa. This phenomenon was improved by the increased pressure value. Under gas pressure of 0.75 Pa and 1.25 Pa, we achieved satisfiable vertical profiles of airholes. Since in nanofabrication process by dry etching technique, a higher pressure may have initiated sputter desorption of the reactive plasma species prior to reaction, thereby leading to the undesirable effects such as reduced etching rate and increased residues. We optimized the gas pressure to the moderate lower value of 0.75 Pa.

We subsequently carried out the investigation on the roles played by gas ratio. The starting condition is the same as condition 1. We fixed the flux of CF_4 to 5 cc and changed that of Ar in order to achieve different gas ratio. This is because during the dry

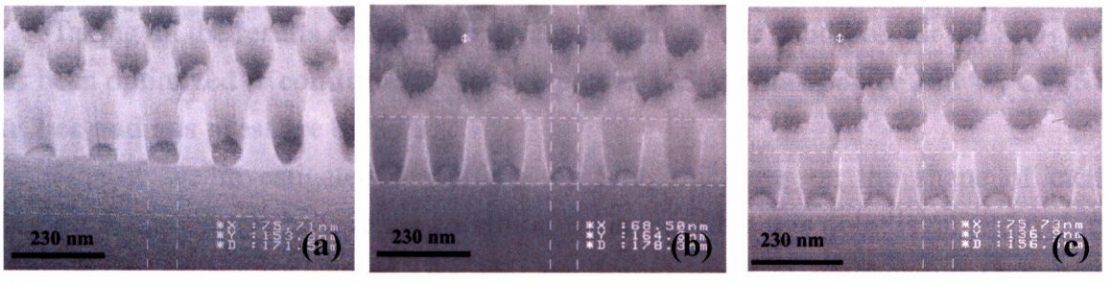

Fig. 4.8 Cross-sectional SEM images of the SiO2 masks fabricated under different CF_4 ratio: (a) 38%, (b) 71% , and (c) 100%. The periodicity is 150 nm and the r/a ratio is 0.3 for (a) and 0.25 for (b) and (c).

etching the etching rate is mainly determined by the etching gas that dominates the chemical etching part. Figure 4.8 shows the cross-sectional images of the fabricated SiO_2 masks under different gas ratios. We define the gas ratio as the percentage of reactive CF_4 gas, the values of which are (a) 38%, (b) 71% and (c) 100%. All the three samples share the common periodicity of 150 nm and the r/a ratio value of 0.3 for (a) and 0.25 for (b) and (c). One can observe that a tiered etch profile with vertical striations in the sidewall was formed under CF_4 ratio of 31%. This phenomenon was improved with the increasing CF_4 ratio by reducing the fulx of Ar additive gas. This can be explained by the understanding of physical and chemical part in dry etching process. In this

etching process, CF_4 plays the role for chemical etching part and Ar additive gas performs the physical etching part. In the chemical part, the etching proceeds as chemical reactions occur on the sample surface. This chemical part is highly isotropic, we can resemble this as the wet etching by chemical solutions. On the other hand, in the physical part, the accelerated ions bombard randomly the sample surface and if the ions have high enough energy, they can knock atoms out of the material to be etched without a chemical reaction. This physical part is highly isotropic. And by changing the balance it is possible to influence the anisotropy of the etching profiles, which is exactly what we have observed in fig. 4.8. In fig. 4.8 (a), the excessive supply of Ar gas (8 cc) yield strong bombardment to the sample, causing the erosion of photoresist. Also the energetic ions scattering from the surface could strike the sidewalls with significant momentum thus increasing the likelihood of increased damage. When we decreased the supply of Ar to 2 cc (SEM image shown in fig. 4.8 (b)), the vertical striations damage in the sidewall completely vanished. Also we achieved good abruptness of the airholes. When we introduced merely CF_4 gas into chamber, no significant difference appeared to the vertical profile of etched sidewalls, instead we got much slower etching rate (65 nm/min in (b) compared to 54 nm/min in (c)). This is due to the absence of physical etching that helps remove the nitrides as well as the etching residues.

Taking all the results and trends into consideration, our condition for the SiO_2 mask has been optimized to **condition 2**: **Source power 125 W, bias power 300 W, CF_4 5 cc, Ar 2 cc and gas pressure 0.75 Pa**.

Finally, we investigated the effects of SiO_2 thickness on the shape of etched airholes. Although we believe the condition we achieved at this point is quite developed compared to where we started. We still get some extent of degradation thought the etching. Declination is yielded to the sidewall of airholes, causing the decrease of airhole diameter in the bottom. This may be fatal to the subsequent III-nitrides etching. As mentioned in the beginning of this section, SiO_2 with thickness values of 130 nm, 195 nm and 260 nm were investigated. Condition 2 was employed as etching condition. Table 4-1 shows the value of the diameters measured at the bottom of the airholes with periodicity of 140 nm, 150 nm and 160 nm. The clear trend can be observed is that the diameter decreases as the thickness of SiO_2 mask increases. This is reasonable since thicker SiO_2 mask means more significant degradation yielded during the process.

As the conclusion to this section, we carried out a systematic investigation of the etching parameters of source power, bias power, gas pressure and gas ratio during the RIE etching of SiO_2 and the optimal condition is concluded as following:

***Optimal condition for the fabrication of SiO_2 mask*:**

Source power 125 W, bias power 300 W, CF_4 5 cc, Ar 2 cc and gas pressure 0.75 Pa.
***Optimal thickness of SiO_2 mask*:**
130 nm

SiO_2 thickness / Periodicity	130 nm	195 nm	260 nm
140 nm	93	70	50
150 nm	83	70	57
160 nm	86	80	70

Table 4-1. Dependence of airhole diameter on SiO_2 thickness. SiO_2 masks with thickness of 130 nm, 195 nm and 260 nm were used for investigation

4.6 Etching of III-Nitride

We subsequently carried out the optimization for the etching condition of AlN layers. We used gas mixture consisting of Cl_2 / Xe or Cl_2 / Ar as etching gas. This part is the last part for our dry etching optimization and is also the essential part. Since recent reports on the fabrication of III-nitrides two dimensional photonic crystals have been mainly focused on the structures with very low Al contents, little is known to the fabrication of AlN-based PCs with periodicity of 150 nm or even smaller. This makes our work very challenging. The optimal fabrication condition for III-nitrides should fulfill the following condition:

1. Abrupt vertical etching profile of the airhole.
2. Small size fluctuation of airhole diameter.

We started from the following condition defined as **condition 1**, which is the conventional condition for III-nitrides etching until then:

Source power 300 W, bias power 100 W, Cl_2 1 cc, Xe 0.3 cc and gas pressure 0.5 Pa

During the whole etching processes, the gas pressure was maintained at the very low level of 0.5 Pa to enhance the anisotropic etching of AlN and suppress the damage of SiO_2 mask.[57,58] The gas ratio, the source power and the bias power were varied to study the influences of these parameters on the etched airhole profiles and aspect ratios.

We first fixed the mixed gas flow at Cl_2 (1 cc) / Xe (0.3 cc) and varied the source and bias powers. The increase of bias power from 100 W to 300 W with common source power of 300 W improved the vertical profiles of airholes remarkably. The inclination angle of airhole sidewall to the substrate calculated by SEM observation revealed the values of 62 and 70 degree, respectively. However, we observed that the diameters of airholes exceeded the designed values significantly with a factor of 50%. This is due to the isotropic etching caused by the increase in both reactive chlorine concentration and the ion density, which is mainly controlled by the source power. We therefore increased the bias power to 500 W, which reaches the maximum of our equipment and investigated the influences of source power systematically in the low source power regime. Graph 4-1 shows the dependence of the airhole sidewall inclination angle on

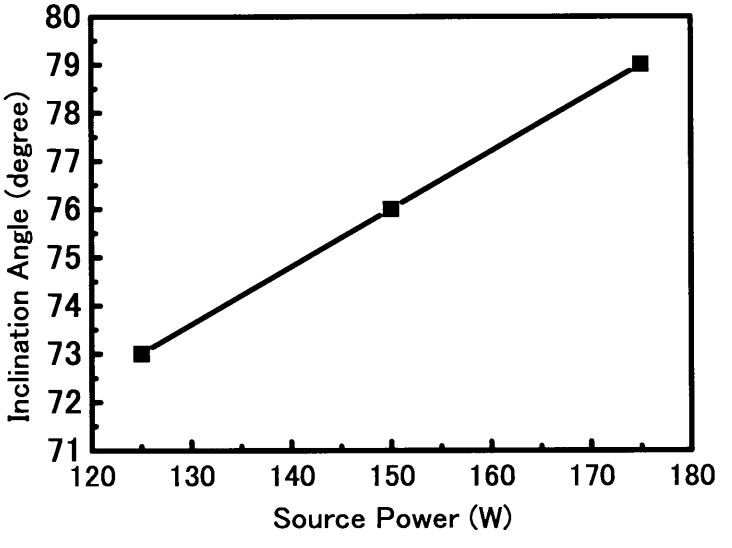

Graph 4-1 Effect of source power on inclination angle of airhole sidewall to substrate. The bias power, etching pressure, etching gas flow rate were maintained as 500 W / 0.5 Pa / Cl_2 (1 cc) / Xe (0.3 cc).

source power. One can observe that the abruptness of airholes was remarkably improved

under high bias power and moderate low source power environment. On the other hand, SEM observation revealed that the etching profile fluctuates significantly upon the different positions of photonic crystal structure. We consider this phenomenon due to the fluctuation of etching gas flow rate that became distinguishing under a very low supplied condition.

Taking these experimental results into consideration, we increased the total flow rate of etching gas by a factor of 5 with the same gas ratio. The AlN etching was subsequently performed under an introduction of Cl_2 (5 cc) / Ar (1.5 cc) instead of Cl_2 / Xe due to the limitation of our equipment. Source power was increased to 200 W expecting better vertical etching profile of the airholes. As the result, excellent abruptness with the inclination angle of 85 degree was obtained with good uniformity. We subsequently fixed the flow rate of Cl_2 to 5 cc and varied the gas ratio of Ar additive gas to investigate its influence on etching profile. Graph 4-2 shows the dependence of airhole sidewall inclination angle on Ar gas ratio. The employment of Ar additive gas with moderate ratio enhances the anisotropic etching of AlN due to its physical etching, however further addition will result in the damage of sample caused by ion bombardments. Note that this phenomenon was also observed in the investigation of SiO_2 mask fabrication. Hence, we presume the following condition as the best to realize

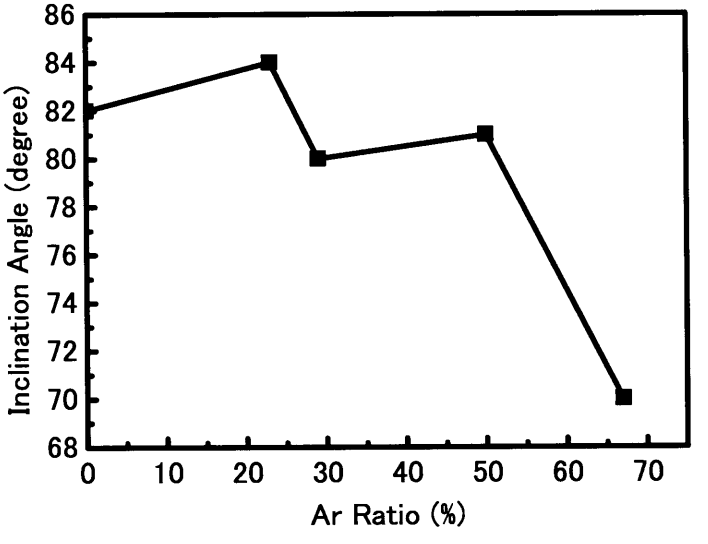

Graph 4-2 Dependence of airhole sidewall inclination angle on additive Ar gas ratio with common condition: Source power 200 W / bias power 500 W / gas pressure 0.5 Pa / Cl_2 5 cc.

vertically abrupt etched profiles:

***Optimal condition for the etching of III-nitrides*:**

Source power 200 W, bias power 500 W, Cl_2 5 cc, Ar 1.5 cc and gas pressure 0.5 Pa.

Figure 4.9 (a) and (b) show the typical SEM images of photonic crystal fabricated under our optimum process. Abrupt vertical etching profiles were obtained to the structure with airhole / periodicity as small as 75 / 150 nm and r/a ratio of 0.25. The etching proceeded to the SiC substrate, revealing the aspect ratio as high as 3. Besides, it is very interesting that hexagonal shaped airholes were achieved in spite of the circular patterns in the SiO_2 mask with excellent reproducibility. This observation is

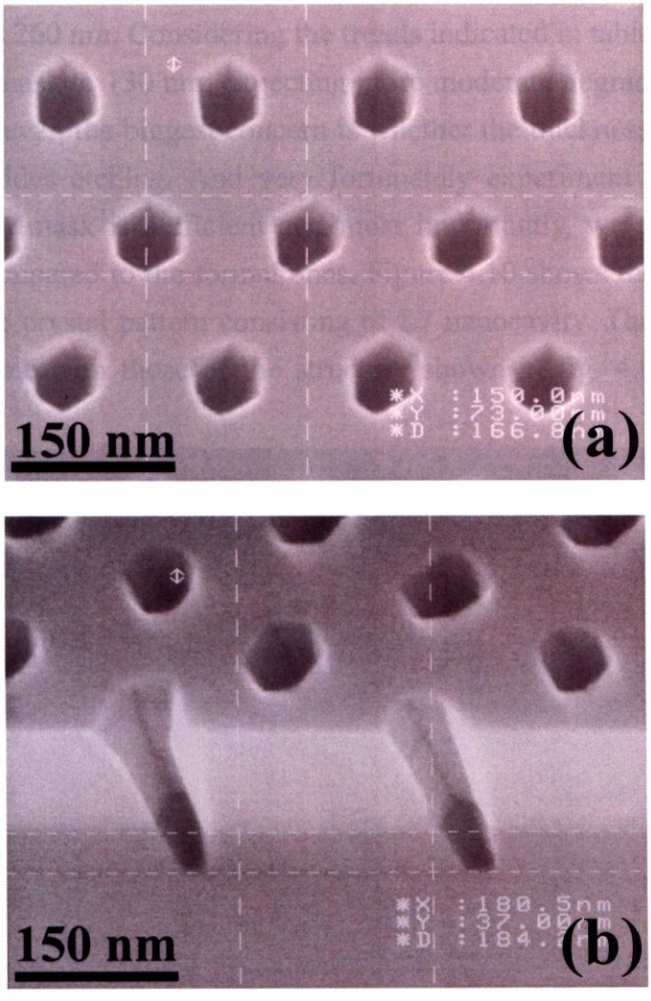

Fig. 4.9 Typical SEM images of 2D PC with periodicity of 150 nm and r/a ratio of 0.25: (a) Top view, (b) Cross-sectional view. Our optimal nanofabrication process promises accurate fabrication of designed patterns and abrupt vertical etching profile even to the structure with periodicity as small as 150 nm.

totally new and no similar results have been reported in former studies. Although the

mechanism behind is still unclear, we consider this might be either due to the effect of chemical etching under our condition or the high Al content of our samples (all the former studies were carried out utilizing samples of a very low Al contents). Further systematic investigation is required on this issue. However, this result is very useful since the high aspect ratio and abrupt vertical profile obtained in our study may be in some respects attributed to this "self-assemble like" hexagonal shape of the airholes.

Although good vertical etching profile has been achieved at this point, we found ourselves facing a new problem. SEM observation revealed that in spite of the designed r/a ratio of 0.25, the diameter of the fabricated airhole is merely 68 nm to the periodicity of 150 nm. Note that the thickness of SiO_2 mask used in all the experiments carried out until this stage was 260 nm. Considering the trends indicated in table 4-1, we change the thickness of SiO_2 mask to 130 nm, expecting more moderate degradation caused during SiO_2 etching. However, the biggest concern is whether the thickness is sufficient for the subsequent III-nitrides etching. And very fortunately experiment results showed that 130 nm thick SiO_2 mask is sufficient and most importantly, we could achieve much bigger diameter compared to the formal ones. Figure 4.10 shows the SEM image of the fabricated photonic crystal pattern consisting of L7 nanocavity. The periodicity and r/a are exactly the same with those of the structure shown in fig. 4.9. SEM observation

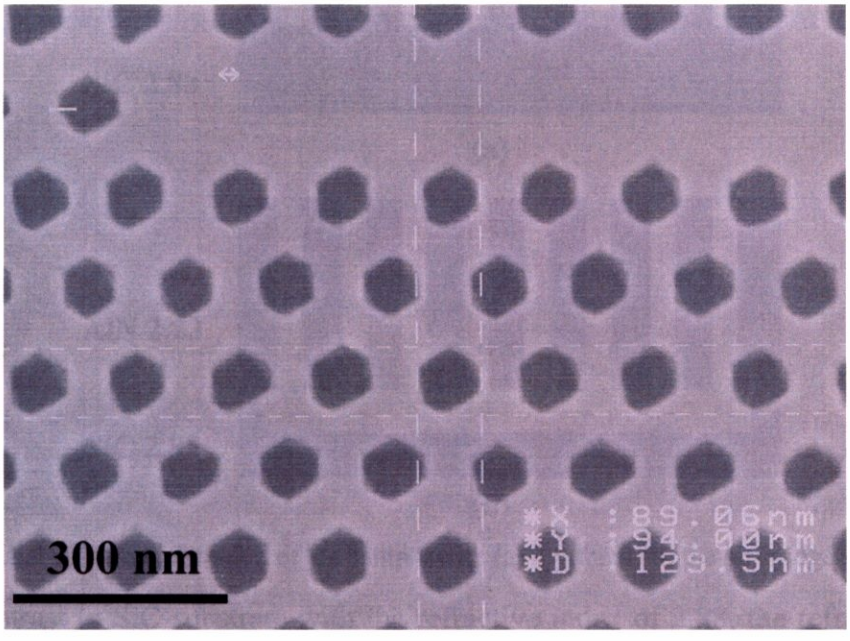

Fig. 4.10 Top view of PC with periodicity of 150 nm and r/a = 0.25 fabricated with 130 nm thick SiO_2 mask.

reveals that we achieved the diameter value of approximately 86 nm after the decrease

of SiO_2 mask compared to the value of 66 nm in the formal structure. This improvement is important since as shown in chapter 2, the r/a ratio yield significant influence on the photonic bandgap. For example, to achieve bandgap around the emission wavelength range of GaN QDs, the periodicity of 150 nm is sufficient for r/a ratio of 0.28(2r = 86 nm). However, the periodicity of 130 nm is essential for r/a ratio of 0.22 (2r = 66 nm), which is extremely difficult to realize.

4.7 Fabrication of Air-Bridge Structure by Photoelectrochemical Etching of SiC

In the former sections, we established the optimal etching process for SiO_2 mask and III-nitrides materials with periodicity of 140 nm. However, one significant problem emerges considering the optical characteristics of our sample structure. As shown in fig.

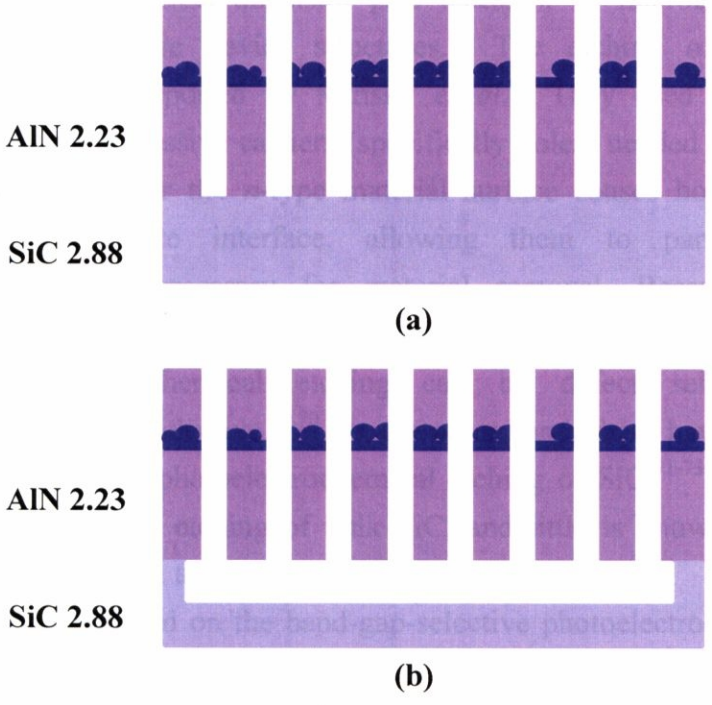

Fig. 4.11 Schematic demonstration of the sample with (a) / without (b) the air-bridge structure.

4.11, in contrast to SiC substrate with the refractive index of 2.88, the refractive index of the III-nitrides layer consisting of GaN QDs is 2.23. This fact is extremely undesirable during the optical experiment. Since the luminescence from QDs will leak into substrate significantly, eventually resulting in the very poor efficiency of light enhancement.

To solve this problem, it is natural for one to propose the introduction of air sacrifice layer between III-nitrides layer and SiC substrate, which is common in the other III-V semiconductor material systems such as GaAs and InP. However, this means we have to etch the SiC substrate, which is an extremely difficult task to accomplish due to its chemically stability and resistance to conventional wet etchants. The most widely used and reliable method for the etching of SiC is the dry etching technique. However, in this study wet etching is essential due to the required etching selectivity and most moderate damage yield to the fabricated III-nitrides photonic crystal structure. Considering the above-mentioned limitation, we employed the method of photoelectrochemical wet etching technique for the etching of SiC.

The goal of this study is to establish the suitable fabrication process for the air-bridge III-nitrides photonic structure by the photoelectrochemical etching of SiC. On the other hand, very recently it has attracted a lot of attention as a useful processing technique for the III-nitrides systems. The photoniduced etching technique has been used extensively for defect delineation,[59,60] as well as creating GaN metal-semiconductor field effect transistor gate recesses,[61,62] microelectromechanical structures,[63,64] and electronic device structures.[65] The etching of GaN utilizing photoelectronic was first reported by Minsky *et al.*[66] They used above band-gap illumination to generate excessive carriers (specifically holes) needed to etch GaN and its alloys. Bandbending near the *n*-type material surface causes holes to be drawn toward the GaN-electrolyte interface, allowing them to participate in the electrochemical reactions necessary for material removal. Because the etching mechanisms rely significantly on the absorption of incident light and surface bandbending, photoelectrochemical etching can be defect selective,[59] dopant selective,[67,68] and band-gap selective.[69,70] On the other hand, there have been very few reports published about the photoelectrochemical etching of SiC.[71-73] But all of these reports were focused on the etching of bulk SiC, and little is known to the etching process especially subsequent to the nanofabrication.

In this study, we focused on the band-gap-selective photoelectrochemical etching of SiC. The biggest hurdle of this study is that the etching of SiC has to been carried out after the fabrication of III-nitrides photonic crystal patterns. We have to pursue the rapid etch rates and smooth etching morphology of SiC as well as assuring the most moderate damage yielded to the photonic crystal patterns above it.

Figure 4.12 shows the apparatus for the photoelectrochemical etching of SiC. The

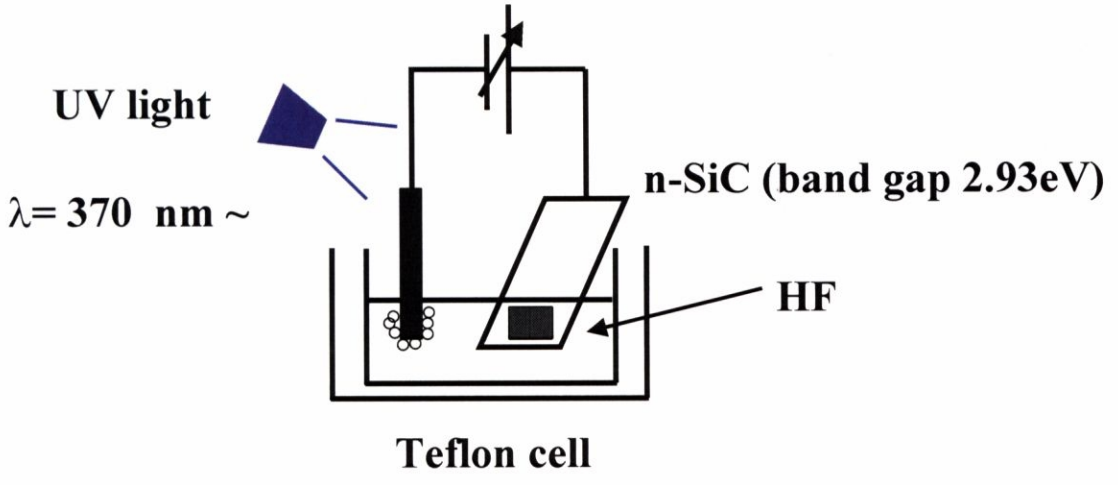

Fig. 4.12 Experimental apparatus for the photoelectrochemical etching of SiC.

etching of SiC was performed at room temperature. Instead of the samples consisting of GaN QDs, metalorganic chemical vapor deposition (MOCVD)-grown AlN layers on n-type (0001)-oriented 6*H*-SiC substrates were first used to carry out the etching of SiC. Using SiO_2 as mask, Cl_2 RIE etching was employed to etch patterns into the epitaxial layers. A part of the sample was subsequently carefully set into the Teflon cell containing hydrogen fluoride (HF) solution. The pH value of electrolyte solution was controlled by the concentration of HF in the pure water. A 200 nm thick Ni and Au was evaporated to the backside of the sample to serve as the electrical contact to the SiC material. During the etching process, ultraviolet light from a mercury lamp was irradiated to generate hole carriers near the n-type SiC surface. Since the band gap of SiC and AlN are 2.93 eV and 6.4 eV respectively, we used a filter that cuts off the light with wavelength shorter than 370 nm to prevent light with energy higher than that of AlN to irradiate on samples. A voltage was applied to enhance the etching rate. Sample and Pt electrode were employed as positive and negative electrode, respectively. Surface morphology, etching residues and etching rate were evaluated by optical microscope and SEM observation.

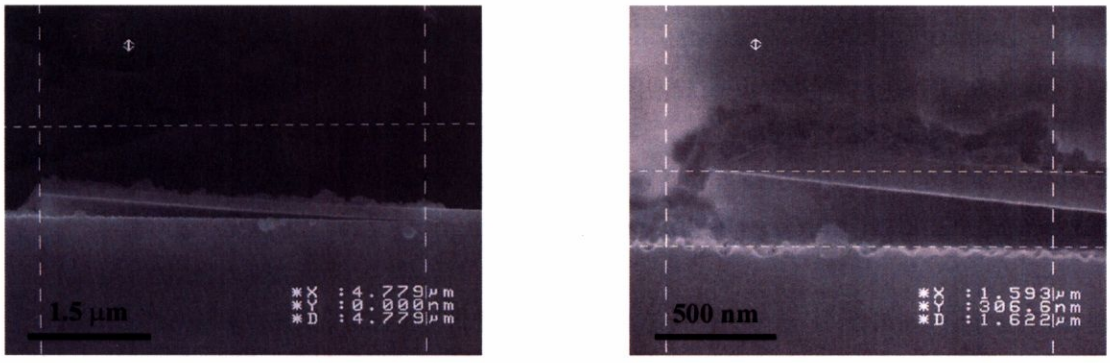

(a) **(b)**

Fig. 4.13 Cross-sectional SEM images of sample after photoelectrochemical etching of SiC. The sample consists of several micrometer-wide AlN waveguide structure.

As mentioned above, since all the reported work were limited on the photoelectrochemical etching of SiC bulk substrate for the purpose of defects evaluation. We did not even know if it is possible to fabricate the air-bridge structure with smooth morphology sufficient for optical characterization. As the first attempt, we used sample containing AlN waveguide structure with the width of several micrometers. The density of HF solution was set to be 0.1%. Figure 4.13 (a) and (b) show the cross-sectional SEM images of the fabricated sample with different magnifications. One can observe the cambering shape on the edge of the waveguide structure, indicating the proceeding of SiC etching. Achieving the feasibility of this method, we fabricated samples consisting of AlN photonic crystal patterns with periodicity ranging from 150 nm to 360 nm. The sample was etched in 0.1% HF solution under the irradiation of UV light for one hour. During the etching process, we observed significant bubbles generating from both sample surface and Pt electrode. Although the mechanism of the reaction going on during the photoelectrochemical etching of SiC is still uncovered, we consider the following reaction may occur to SiC serving as the positive electrode.

$$Si + h^+ + 2OH^- \rightarrow SiO_2 + H_2 \quad \cdots\cdots\cdots (1)$$

The oxidized SiO2 subsequently dissolves in HF solution, leading to the removal of SiC. The C atom may become CO2 or CO gas during the etching process but the mechanism is not yet clarified. And again although uncertain we think the bubbles generated near the negative electrode is H_2 gas due to the reduction reaction of H^+ in the electrolyte.

Figure 4.14 (a) and (b) show the SEM image of the etched sample. Fig. 4.14 (a) reveals that the etching of SiC proceeded to such an extent that the adjacent patterns have communicated with each other. This once again proves the feasibility of SiC etching utilizing photoelectrochemical etching. However, this elementary experiment

also revealed two problems to be solved:

1. The photoelectrochemical etching of SiC is an extremely isotropic etching process, thus the arrangement of photonic crystal patterns has to be designed considering this feature.
2. Significant etching residue remains both on the sample surface and inside the airholes. The extreme roughness yielded to the sample is fatal upon optical characterization.

To be more specific, we should not forget the general isotropic feature of wet

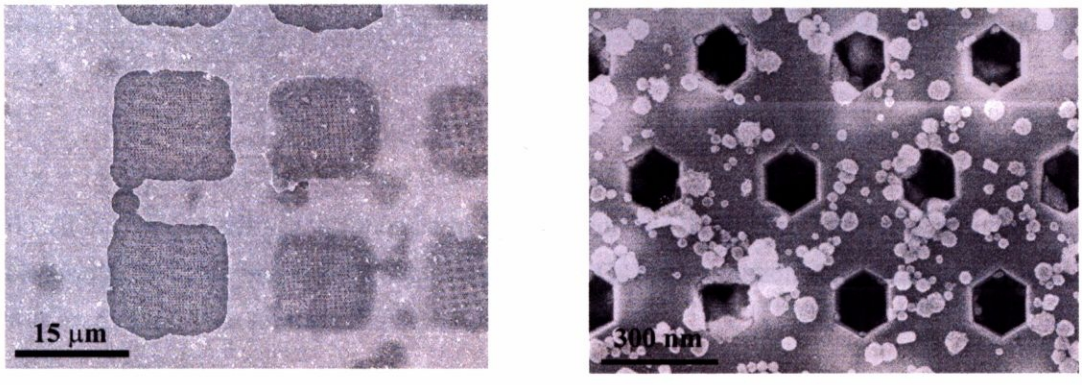

(a) **(b)**

Fig. 4.14 SEM images of the etched sample consisting of AlN photonic crystal patterns. In fig. 4.14 (a), the membrane containing photonic crystal patterns were removed due to the proceeding of the wet etching. Fig. 4.14 (b) shows the significant etching residues remaining on the sample surface.

etching technique, and the arrangement, especially the intervals between each pattern has to be designed considering this issue. And as shown in fig. 4.14 (b), the significant rough etching morphology due to the huge amount of residues will yield fatal negative influence to the optical experiment. In another way, the etching process has to be greatly improved otherwise we could not expect any optical characteristics due to the existence of photonic crystal in this stage.

As the improvement to etching process, we first designed the interval between each pattern to be 70 μm instead of the former value of approximately 25 μm shown in fig. 4.14. The second problem is much more difficult to solve since we do not know the component of the etching residues. By recalling the whole fabrication process we have come through, one possible concern is the grease used in RIE etching. Since this grease could not be completely removed by our conventional rinse procedure. And of course, many other possibilities may account. As the attempt, we adopted new rinse procedures prior to and after the etching of SiC, respectively. Prior to the SiC etching, the sample

was rinsed in trichloroethylene followed by IPA solution and terminated in BHF using

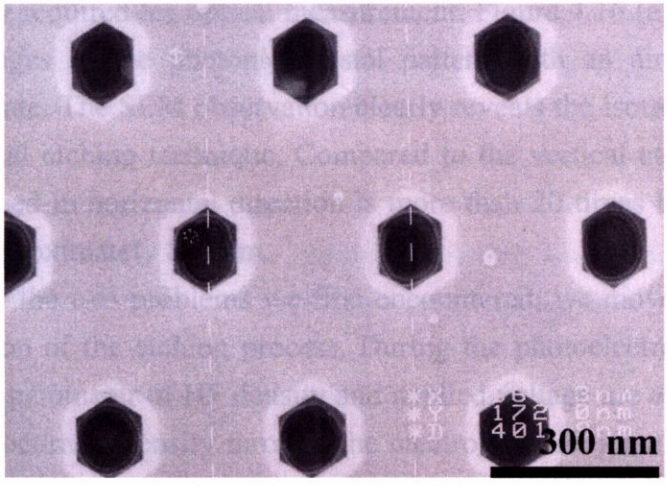

Fig. 4.15 Surface morphology after the photoelectrochemical etching of SiC. The sample was rinsed in trichloroethylene followed by IPA solution and terminated in BHF using ultrasonic cleanser prior to the SiC etching. And a H_2SO4 / H_2O_2 / H_2O solution with the ratio of 1 : 1 : 5 was used to rinse the sample after the SiC etching.

ultrasonic cleanser. This rinse procedure has been proved to be effective to remove the grease adhering to the sample. On the other hand, we employed the well-known rinse method in Si semiconductor utilizing H_2SO4 / H_2O_2 / H_2O solution with the ratio of 1 : 1 : 5 after the SiC etching. Figure 5.5 shows the SEM image of the sample fabricated employing these two procedures. One can observe that the etching residues were drastically decreased yielding the smooth morphology of the etched sample. Note that

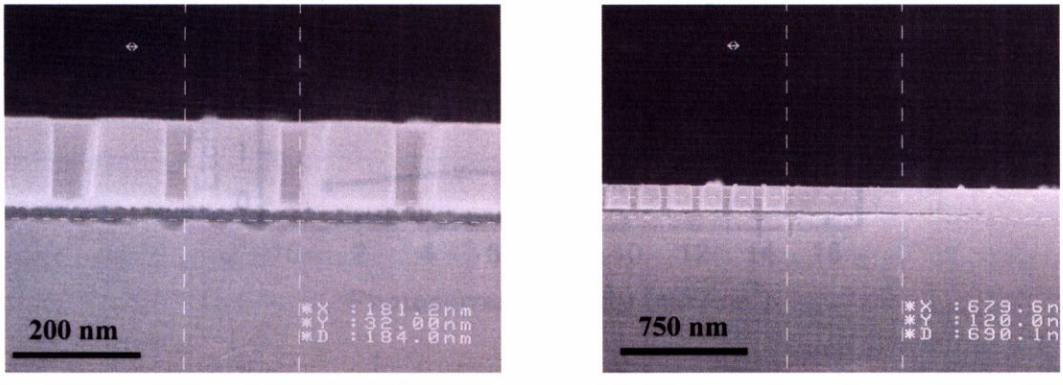

(a) **(b)**

Fig. 4.16 Cross-sectional images of the photonic crystal pattern with air layer introduced between SiC substrate. The periodicity and r/a ratio are 180 nm and 0.25, respectively. A comparison between (a) and (b) reveal the isotropic feature of photoelectrochemical etching.

fig. 4.14 (b) and 4.15 have the common periodicity and r/a ratio of 360 nm and 0.25,

respectively. Therefore we believe these rinse procedures could promise the smooth surface morphology required for optical measurement. Figure 4.16 (a) and (b) show the cross-sectional images of the photonic crystal pattern with an air layer introduced between SiC substrate. The SEM observation clearly reveals the isotropic feature of the photoelectrochemical etching technique. Compared to the vertical etching depth of 32 nm, the etching speed in horizontal direction is more than 20 times faster, yielding the etching depth of approximately 800 nm.

Having solved the two problems we first encountered, we moved on to the more specific investigation of the etching process. During the photoelectrochemical etching process of SiC, the parameter of HF density and applied voltage are essential since they determine the photocurrent density through the electrolyte-SiC junction. Therefore we subsequently changed these two parameters throughout a wide range and investigated their influence on the etching rate and etching morphorlogy systematically. We first fixed the HF density to 0.1% and changed the parameter of photocurrent density value between 1 mA / cm^2 and 15 mA / cm^2 by applying different voltages on sample surface. The etching time was set to 30 min for the whole optimization experiments. The etching

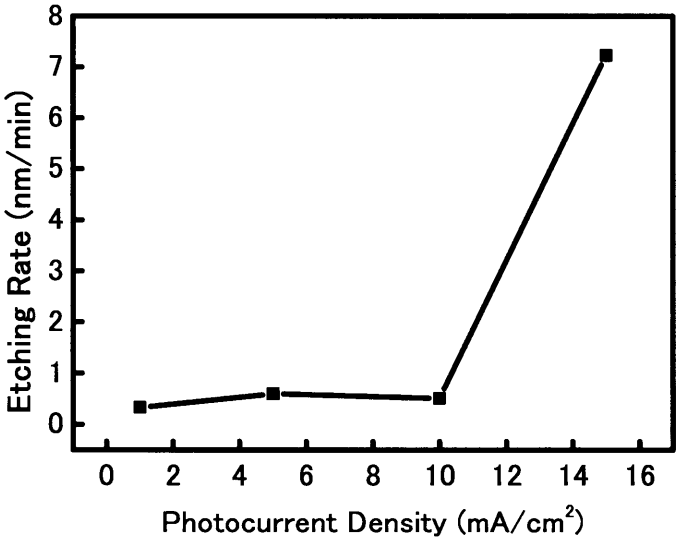

Graph 4-3 Dependence of etching rate on photocurrent density.

rate was determined by SEM observation. Graph 4-3 shows the dependence of etching rate on photocurrent density. We found no significant change in etching rate under the photocurrent density of 1, 5 and 10 mA / cm^2, however when we increased the photocurrent density to 15 mA / cm^2 by tuning the applying voltage, we found a big jump from below 1 nm / min region to 7 nm / min. Although we could not explain the

clear reason for this big jump, a glance of reaction equation (1) shown before could help us to understand. During the etching of SiC, Si atom is first oxidized and subsequently dissolves in the HF solution. And the oxidization of Si requires holes generated by the irradiation of ultraviolet light. An increase of applied voltage will gather holes near sample surface. This will make the holes easier to participate the reaction, eventually results in the enhanced etching rate.

We subsequently fixed the photocurrent to 15 mA / cm^2 and investigated the effects of HF density. No significant improvement on etching rate has been observed. Besides,

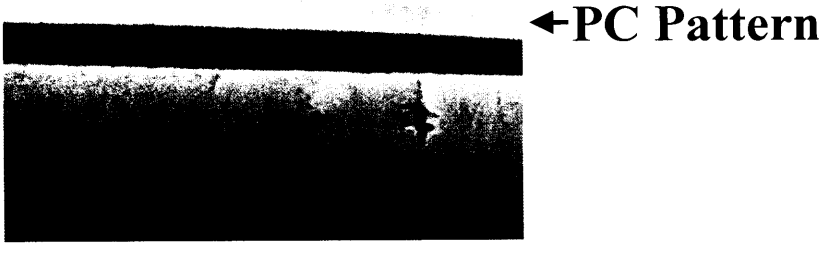

Fig. 4.17 Cross-sectional images of AlN photonic crystal consisting of a 215 nm thick air-bridge structure. The periodicity of r/a ratio are 170 nm and 0.325 respectively.

we found the etching process became fierce companied by a great amount of bubbles surging on the sample surface. Considering the possible deterioration to etched morphology yielded by the perturbation. We chose the more unperturbed condition of low HF density as the optimal etching condition for the photoelectrochemical etching of SiC. Figure 4.17 shows the cross-sectional SEM image of the sample fabricated under this condition. The periodicity and r/a ratio of the sample are 170 nm and 0.325, respectively. An air-bridge structure was successfully introduced between the AlN photonic crystal membrane and SiC substrate. The thickness of air layer is approximately 215 nm. Moderate smooth etching morphology was also achieved.

4.8 Conclusion Remarks

In this chapter, the systematic investigation for the most suitable fabrication process for two-dimensional III-nitrides photonic crystal has been specified. As demonstrated in section 4.1, our structure requires periodicity of 150 nm or even smaller.

To realize this goal especially in III-nitrides material system, the most reliable technique are EB lithograph and dry etching. After introducing the mechanism and specification of our RIE equipment in section 4.2, we moved on to the optimization experiments following the procedure shown in section 4.3. The details of the investigation and the optimal conditions for the photoresist developing, SiO_2 mask fabrication and III-nitrides etching are demonstrated in the following section 4.4, 4.5 and 4.6 respectively. The optimal condition for the fabrication of SiO_2 mask is conclude as following:

***Optimal condition for the fabrication of SiO_2 mask*:**

Source power 125 W, bias power 300 W, CF_4 5 cc, Ar 2 cc and gas pressure 0.75 Pa.

***Optimal thickness of SiO_2 mask*:**

130 nm

With the alternate supply of 2 cc O_2 gas for 5 seconds with a time interval of 50 seconds.

***Optimal condition for the etching of III-nitrides*:**

Source power 200 W, bias power 500 W, Cl_2 5 cc, Ar 1.5 cc and gas pressure 0.5 Pa.

Using the process optimized above, we could fabricate two-dimensional III-nitrides photonic crystals with abrupt vertical profiles, high aspect ratio (~3) and excellent reproducibility even to the structure with periodicity as small as 140 nm and 150 nm. We could fabricate periodicity as small as 140 nm and 150 nm to the structure with r/a ratio of 0.3 and 0.325, respectively.

In the following section 4.7, the fabrication of air-bridge structure utilizing photoelectrochemical etching of SiC has been demonstrated. The very few reported study on the photoelectrochemical etching of SiC made our study extremely challenging. On the other hand, this procedure is essential since the leaky waveguide structure due to the refractive index profile is fatal upon optical characterization. By optimizing the etching parameters of HF density and photocurrent as well as solving the unexpected hindrance such as the procedure of sample rinse, we successfully fabricated the air-bridge structure with thickness bigger than 200 nm. However, further improvement is required to the etching process:

1. In the current apparatus, Au coated clip was used to fix the sample and serve as the electrode at the same time. We have to always set the sample very carefully keeping the clip away from HF solution. One can imagine how exhausting this task will be since the sample area is merely 6×6 mm^2. And it really makes you upset when you find the sample is completely ruined simply due to a slightly dip of the clip into the HF solution. Also, the

very primitive way of using clip as electrode is far from satisfaction. We may use EB evaporation to deposit HF-proof materials on sample surface as electrode. Some further investigation is required upon this issue.

2. The reproducibility of etching rate needs to be improved. Stirring the solution during etching process may be a good solution. However, as mentioned above the evolution of our experimental apparatus is the biggest priority.

Although there still remains some challenging assignments, this work was absolutely an important and successful attempt for the fabrication of III-nitride air-bridge photonic crystals.

In summary, the optimal condition is concluded as following:

***Optimal condition for the photoelectrochemical etching of SiC*:**

HF density 0.1%, photocurrent density 15 mA / cm^2

Etching rate:

~ 7 nm / min.